ChemComm

COMMUNICATION

The effects of conformation on the noncovalent bonding interactions in a bistable donor–acceptor [3]catenane†

Cheng Wang,[a] Dennis Cao,[ab] Albert C. Fahrenbach,[ab] Sergio Grunder,[a] Sanjeev K. Dey,[a] Amy A. Sarjeant[a] and J. Fraser Stoddart*[ab]

A switchable donor–acceptor bistable [3]catenane, composed of a crown ether containing a pair of alternating π-electron rich tetrathiafulvalene and 1,5-dioxynaphthalene units, encircled by two π-electron deficient cyclobis(paraquat-*p*-phenylene) rings, has been synthesised and the redox-activated switching it undergoes investigated.

In nature, biological systems can spontaneously convert[1] chemical into mechanical energy by using sophisticated motor molecules to conduct stepwise linear or rotary molecular-level motions. These motors play essential roles in a wide variety of events, important for sustaining life, particularly those related to the activities in cells, *e.g.*, ATP synthesis.[2] All of these motors rely on a cocktail of molecular recognition processes that involve a subtle interplay between inter- and intramolecular noncovalent bonding interactions in order to execute their biological functions. In order to help unravel the complexities of their intramolecular geometries and interactions, and the recognition processes behind them, not to mention engineer totally synthetic prototypes, researchers have been inspired to develop so-called artificial molecular machines[3] which are designed to exploit the same types of noncovalent bonding interactions found in naturally occurring motor molecules. Towards this end, molecular switches,[4] elevators,[5] rotors,[6] and muscles[7] have been reported.

In the realm of artificial molecular switches,[3] mechanically interlocked molecules (MIMs),[8] such as bistable catenanes and rotaxanes,[9] are particularly well-suited for nanomechanical work and have gained[9] much attention during the past two decades. The controllable co-conformational molecular motions—circumrotation and translation—displayed within MIMs have found many applications in molecular electronic devices[10] (MEDs), mechanised mesoporous silica nanoparticles (MMSNPs) for drug delivery,[11] and nanoelectromechanical systems[12] (NEMS).

[a] *Center for the Chemistry of Integrated Systems, Department of Chemistry, Northwestern University, 2145 Sheridan Road, Evanston, IL 60208, USA. E-mail: stoddart@northwestern.edu; Fax: +1-847-491-1009; Tel: +1-847-491-3793*
[b] *NanoCentury KAIST Institute and Graduate School of EEWS (WCU), Korea Advanced Institute of Science and Technology (KAIST), 373-1, Guseong Dong, Yuseong Gu, Daejeon 305-701, Republic of Korea*
† Electronic supplementary information (ESI) available: Synthesis and characterisation. CCDC 886394. For ESI and crystallographic data in CIF or other electronic format see DOI: 10.1039/c2cc34190e

For example, bistable [2]rotaxanes have been employed[10a] in the fabrication of a working defect-tolerant 160 kBit molecular memory device with a density of 10^{11} bits per square centimeter.
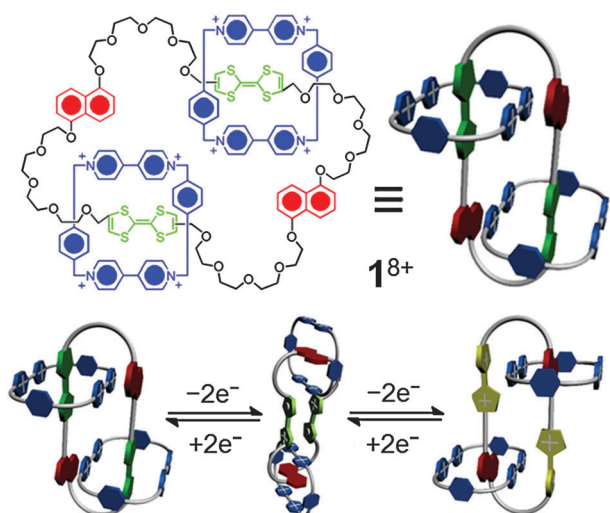
Tetrathiafulvalene (TTF), on account of its two reversible oxidation processes, has proven[13] to be an indispensable building block for materials chemists. On account of the much stronger binding of TTF to cyclobis(paraquat-*p*-phenylene) (CBPQT^{4+}), compared to that of 1,5-dioxynaphthalene (DNP), TTF has been incorporated into bistable MIMs along with DNP to construct redox-active molecular switches.[10b] In 1998, we reported[9a] a bistable [2]catenane which is composed of a crown ether containing π-electron rich TTF and DNP recognition units, interlocked mechanically with a CBPQT^{4+} ring. The switching is controlled by the reversible oxidation and reduction of the TTF unit. These redox processes induce the translational movement of CBPQT^{4+} ring between the TTF and DNP units. The ground-state distribution of translational isomers favours[14] encirclement of the TTF unit—called the ground state co-conformation (GSCC)—over the DNP unit—called the metastable state co-conformation (MSCC)—in a 150 : 1 ratio, while in its linear rotaxane analogue, the distribution is over an order of magnitude less at 10 : 1. This difference in ratios prompted us to speculate that the geometry of the catenane leads to enforced noncovalent bonding interactions—namely, preorganisation[15] in the molecular world of the mechanical bond—which amplify the stability of the TTF-encircled translational isomer in comparison with the rotaxane. Thus, we became interested in exploring this switching behaviour, and in particular, the ground-state distribution of translational isomers, of the bistable [3]catenane $\mathbf{1}^{8+}$ (Scheme 1), in which the crown ether **2** (see ESI†) containing two TTF units and two DNP units is interlocked mechanically with two CBPQT^{4+} rings. Here, we report (1) the template-directed synthesis of $\mathbf{1}^{8+}$, (2) its solid-state structure and superstructure, and (3) its switching behaviour in solution. As a consequence of the conformation of the crown ether, the arrangement of the multiple noncovalent bonding interactions resembles more closely those found in the corresponding [2]rotaxane rather than the [2]catenane, containing in each case only one set of TTF and DNP units in their polyether components, leading to a ground-state distribution of 10 : 1 in $\mathbf{1}^{8+}$.

The template-directed synthesis of [3]catenane $\mathbf{1}\cdot 8PF_6$ is outlined in the ESI.† Slow diffusion of $^{i}Pr_2O$ into a MeCN solution of $\mathbf{1}\cdot 8PF_6$ produced[17] dark green crystals, suitable for

Scheme 1 Structural formula for the bistable [3]catenane 1^{8+}, which contains two TTF and two DNP recognition units as well as two $CBPQT^{4+}$ rings, and a schematic representation of its redox-controlled switching behaviour.

X-ray crystallography. The crystal structure and superstructure are shown in Fig. 1a and b. The TTF units exist in their *trans* configurations within the $CBPQT^{4+}$ cavities and are stabilised by a combination of weak interactions, including π–π stacking between the bipyridinium units and the included TTF units, as well as [C–H···O] close contacts between some of the crown ether oxygens and the bipyridinium α-hydrogens. The DNP units participate in alongside short interplanar π–π stacking interactions with the outside faces of the bipyridinium units, but only interact with half of the bipyridinium units. It is important to note the fact that the [C–H···O] interactions are spread out across both $BIPY^{2+}$ units of the $CBPQT^{4+}$ ring, a feature which is reminiscent of the intramolecular interactions
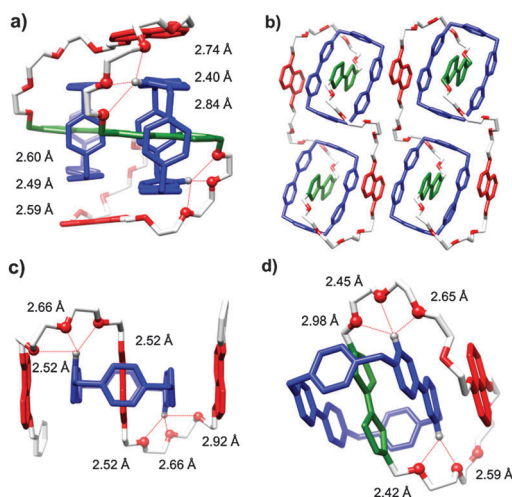

Fig. 1 (a) A plan view of the solid-state structure of 1^{8+} and (b) its superstructure, (c) a plan view of the solid-state superstructure of the [2]pseudorotaxane[16] which serves as a model for the analogous [2]rotaxane, and (d) the solid-state structure of a related [2]catenane.[9a] Note how the [C–H···O] interactions in 1^{8+} resemble those of the [2]pseudorotaxane and not those of the [2]catenane. The disordered PF_6^- counterions, hydrogen atoms and disordered solvent molecules are omitted for clarity.

present (Fig. 1c and d) in the analogous [2]pseudorotaxane[16] and *not* the [2]catenane.[9a] In the analogous [2]catenane, the [C–H···O] interactions are necessarily confined to only one of the $BIPY^{2+}$ units, a condition imposed by the cyclic nature of the crown ether.

In order to study the mechanical movement of the $CBPQT^{4+}$ ring between the TTF and DNP units and evaluate the ground-state distribution of the translational isomers, the switching behaviour of 1^{8+} was investigated (see ESI†) by UV-Vis spectroscopy and cyclic voltammetry (CV) in MeCN. Its ground-state UV-Vis spectrum shows a broad charge transfer (CT) absorption band centered at 830 nm, which is characteristic of the translational isomer in which the TTF unit is encircled by the $CBPQT^{4+}$ ring. The addition of $Fe(ClO_4)_3$ (up to 2 equiv.) causes a continuous decrease in the intensity of the CT band at 830 nm, accompanied by an increase in the intensity of the absorption bands at 450 and 600 nm, which are characteristic of $TTF^{•+}$ radical cation. These observations indicate that the $CBPQT^{4+}$ ring migrates away from the $TTF^{•+}$ to the DNP unit. Interestingly, another two absorption bands, centered on 523 and 785 nm, which also appeared during this process, can be assigned[18] to the characteristic absorption bands of the TTF radical cation dimer $(TTF^{•+})_2$. The intensities of these bands, arising from dimerisation, are approximately half of those observed for the free macrocycle (see ESI†) under identical conditions, leading us to estimate that the equilibrium ratio between the $TTF^{•+}$ radical cation dimer and the free radical species to be about 1 : 1 in the $1^{2(•+)8+}$ catenane. The ability of the oxidised catenane to dimerise is hindered by the energetic penalty of bringing the bulky and positively charged $CBPQT^{4+}$ rings close together. This interaction was not anticipated at the outset. Further addition of $Fe(ClO_4)_3$ until the fully oxidised state was reached resulted in a weak absorption at 525 nm, associated with the CT band between the DNP unit and the $CBPQT^{4+}$ ring. The original spectrum can be recovered following reduction by ascorbic acid, indicating that these redox processes in 1^{8+} are fully reversible.

We have employed variable scan-rate CV in order to measure[14] the distribution of translational isomers in the ground state at equilibrium. The electrochemical behaviour of 1^{8+}, as indicated (Fig. 2) by CV, was also recorded in MeCN at 298 K. In the case of an analogous [2]catenane, the distribution was measured to be 150 : 1, while in the case of the analogous [2]rotaxane, it is 10 : 1. Previously, we invoked the idea of enforced side-on interactions present in the geometry in the [2]catenane while not so in the [2]rotaxane to rationalise this order of magnitude difference in distribution constants. Specifically, the [C–H···O] interactions in the catenane are forced to involve only one $BIPY^{2+}$ unit, whereas in the rotaxane, the [C–H···O] interactions are spread out over these $BIPY^{2+}$ units. We hypothesise that there is a cooperative effect, which results from confining the [C–H···O] interactions to the inside $BIPY^{2+}$ unit that increases the ground-state distribution constant in a non-linear fashion. The concept is analogous to preorganisation, except that it is within the context of the mechanical bond, and so has its basis in the molecular world rather than the *supra*molecular one. This fact makes these intramolecular recognition processes similar to
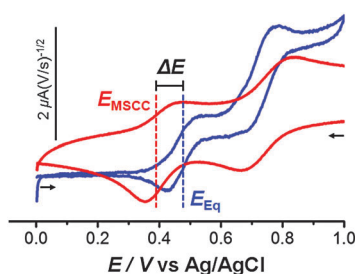
Fig. 2 Cyclic voltammograms of 1^{8+} recorded in the oxidation region in the fast-scan (red trace, 5 V s^{-1}, IR compensated, background subtracted) and the slow-scan (blue trace, 10 mV s^{-1}) rate regimes. Both traces were recorded in argon-purged MeCN (0.5 mM, 0.1 M TBAPF$_6$) at 298 K.

the ones that control, for example, the folded structure of a protein rather than its ability to bind different substrates. In the oxidation region of 1^{8+} recorded in the fast-scan rate regime (200 mV s^{-1}, see ESI†), a small peak is observed around +0.50 V, the intensity of which is commensurate with a 10 : 1 distribution. As the TTF is encircled by CBPQT^{4+} ring, the first oxidation of TTF is shifted to a higher potential. When scanning in the slow scan-rate regime, the degree of the shift in the first oxidation potential of TTF, measurable as E_{Eq}, compared to that of "free TTF" which is measurable in the fast scan rate regime as E_{MSCC}, is used to determine the ground-state distribution ratio of GSCC to MSCC. We confirmed this distribution constant to be 10 : 1 by observing a 60 mV difference between E_{MSCC} and E_{Eq}. Even although 1^{8+} is a catenane, its intramolecular interactions are more in keeping with a [2]rotaxane than those of a [2]catenane, a feature which is reflected in its ground-state distribution at equilibrium.

The switching behaviour of 1^{8+} was also monitored (see ESI†) by ^{1}H NMR spectroscopy in CD$_3$CN at 233 K. In the ground state, the ^{1}H NMR spectrum is further complicated because of (1) the presence of multiple isomers stemming from the cis/trans isomerism of the TTF units and (2) the dynamic processes associated with the CBPQT^{4+} ring. After the oxidation of TTF units, however, with tris(4-bromophenyl)aminium hexachloroantimonate, the ^{1}H NMR spectrum becomes relatively simple. The signals for the TTF unit shift to 9.20 ppm, a δ value which is characteristic of the free TTF^{2+} dication. The DNP protons experienced large up-field shifts to 2.30 (H$_{4/8}$), 5.95 (H$_{3/7}$), and 6.21 (H$_{2/6}$) ppm, respectively, indicating that the CBPQT^{4+} rings have undergone translation from the oxidised TTF units to the DNP units. Subsequent reduction of TTF^{2+} with zinc powder results in the movement of the CBPQT^{4+} rings away from the DNP units and back to the TTF units, restoring the original (ground state) ^{1}H NMR spectrum.

In this communication, we have demonstrated synchronised switching of a bistable [3]catenane during an investigation which provides additional fundamental understanding of switchable MIMs and the effect that their intramolecular interactions have on their ground-state thermodynamics. This knowledge offers new perspectives for further development of MIM-based molecular materials, and has the potential to lead to fresh insights into the complex recognition processes exploited by naturally occurring motor molecules.

Notes and references

1 (a) F. Jon Kull, E. P. Sablin, R. Lau, R. J. Fletterick and R. D. Vale, Nature, 1996, 380, 550–555; (b) M. G. L. van den Heuvel and C. Dekker, Science, 2007, 317, 333–336.
2 P. D. Boyer, J. Biol. Chem., 2002, 277, 39045–39061.
3 (a) A. Coskun, M. Banaszak, R. D. Astumian, J. F. Stoddart and B. A. Grzybowski, Chem. Soc. Rev., 2012, 41, 19–30; (b) E. R. Kay, D. A. Leigh and F. Zerbetto, Angew. Chem., Int. Ed., 2007, 46, 72–191.
4 V. Balzani, M. Clemente-León, A. Credi, B. Ferrer, M. Venturi, A. H. Flood and J. F. Stoddart, Proc. Natl. Acad. Sci. U. S. A., 2006, 103, 1178–1183.
5 J. D. Badjić, V. Balzani, A. Credi, S. Silvi and J. F. Stoddart, Science, 2004, 303, 1845–1849.
6 A. M. Schoevaars, W. Kruizinga, R. W. J. Zijlstra, N. Veldman, A. L. Spek and B. L. Feringa, J. Org. Chem., 1997, 62, 4943–4948.
7 J. Wu, K. C.-F. Leung, D. Benítez, J.-Y. Han, S. J. Cantrill, L. Fang and J. F. Stoddart, Angew. Chem., Int. Ed., 2008, 47, 7470–7474.
8 (a) G. Schill, Catenanes, Rotaxanes, and Knots, Academic Press, New York, 1971; (b) Molecular Catenanes, Rotaxanes, and Knots, ed. J.-P. Sauvage and C. Dietrich-Buchecker, Wiley-VCH, Weinheim, 1999; (c) J. F. Stoddart, Chem. Soc. Rev., 2009, 38, 1802–1820.
9 (a) M. Asakawa, P. R. Ashton, V. Balzani, A. Credi, C. Hamers, G. Mattersteig, M. Montalti, A. N. Shipway, N. Spencer, J. F. Stoddart, M. S. Tolley, M. Venturi, A. J. P. White and D. J. Williams, Angew. Chem., Int. Ed., 1998, 37, 333–337; (b) D. W. Steuerman, H.-R. Tseng, A. J. Peters, A. H. Flood, J. O. Jeppesen, K. A. Nielsen, J. F. Stoddart and J. R. Heath, Angew. Chem., Int. Ed., 2004, 43, 6486–6491; (c) H. Y. Au-Yeung, G. D. Pantoş and J. K. M. Sanders, Angew. Chem., Int. Ed., 2010, 49, 5331–5334.
10 (a) J. E. Green, J. W. Choi, A. Boukai, Y. Bunimovich, E. Johnston-Halperin, E. DeIonno, Y. Luo, B. A. Sheriff, K. Xu, Y. S. Shin, H.-R. Tseng, J. F. Stoddart and J. R. Heath, Nature, 2007, 445, 414–417; (b) A. Coskun, J. M. Spruell, G. Barin, W. R. Dichtel, A. H. Flood, Y. Y. Botros and J. F. Stoddart, Chem. Soc. Rev., 2012, 41, 4827–4859.
11 M. W. Ambrogio, C. R. Thomas, Y.-L. Zhao, J. I. Zink and J. F. Stoddart, Acc. Chem. Res., 2011, 44, 903–913.
12 (a) J. Berná, D. A. Leigh, M. Lubomska, S. M. Mendoza, E. M. Pérez, P. Rudolf, G. Teobaldi and F. Zerbetto, Nat. Mater., 2005, 4, 704–710; (b) Y. B. Zheng, Y.-W. Yang, L. Jensen, L. Fang, B. K. Juluri, A. H. Flood, P. S. Weiss, J. F. Stoddart and T. J. Huang, Nano Lett., 2009, 9, 819–825.
13 (a) J. L. Segura and N. Martín, Angew. Chem., Int. Ed., 2001, 40, 1372–1409; (b) M. Bendikov, F. Wudl and D. F. Perepichka, Chem. Rev., 2004, 104, 4891–4946; (c) D. Canevet, M. Sallé, G. Zhang, D. Zhang and D. Zhu, Chem. Commun., 2009, 2245–2269.
14 A. C. Fahrenbach, J. C. Barnes, H. Li, D. Benítez, A. N. Basuray, L. Fang, C.-H. Sue, G. Barin, S. K. Dey, W. A. Goddard III and J. F. Stoddart, Proc. Natl. Acad. Sci. U. S. A., 2011, 108, 20416–20421.
15 D. J. Cram, Angew. Chem., Int. Ed. Engl., 1988, 27, 1009–1020.
16 P. R. Ashton, D. Philp, N. Spencer, J. F. Stoddart and D. J. Williams, J. Chem. Soc., Chem. Commun., 1994, 181–184.
17 Crystal data for 1·8PF$_6$: C$_{140}$H$_{152}$N$_8$O$_{20}$F$_{48}$P$_8$S$_8$, M_r = 3682.94, 0.093 × 0.044 × 0.038 mm, triclinic, space group P$\bar{1}$, a = 13.9148(6), b = 16.0786(8), c = 21.8368(11) Å, α = 93.109(4), β = 104.124(3), γ = 90.629(3)°, V = 4729.4(4) Å^3, Z = 1, ρ_{calcd} = 1.293 g cm^{-3}. R_{int} = 0.0955, $wR(F_2)$ = 0.3540.
18 I. Aprahamian, J.-C. Olsen, A. Trabolsi and J. F. Stoddart, Chem.–Eur. J., 2008, 14, 3889–3895.